Co-published by
Institute of Fluid-Flow Machinery
Polish Academy of Sciences
Committee on Thermodynamics and Combustion
Polish Academy of Sciences

http://www.imp.gda.pl/archives-of-thermodynamics/

Optimisation of heat pipe heat exchangers with deep cooling of boiler flue gas based on entropy generation minimisation method

Andriy Redko[a], Adam Ujma[b], Oleksandr Redko[c], Ihor Redko[d], Vadym Zadiranov[c*], Vitalii Zaika[c]

[a]Sumy National Agrarian University, Gerasima Kondratieva 160, Sumy 40000 Ukraine
[b]University of Applied Sciences in Nysa, Faculty of Technical Sciences, Armii Krajowej 7, Nysa 48-300, Poland
[c]O.M. Beketov National University of Urban Economy in Kharkiv, Marshal Bazhanov 17, Kharkiv 61002, Ukraine
[d]Ukrainian State University of Railway Transport, Maidan Feuerbach 7, Kharkiv 61001, Ukraine
*Corresponding author email: vadimharij@gmail.com

Received: 14.07.2024; revised: 09.10.2025; accepted: 21.10.2025

Abstract

The paper presents the results of numerical simulations and optimisation of boiler heat exchanger parameters under conditions of deep cooling of combustion products. The specific features of heat and mass transfer calculations, particularly when combustion products are cooled below the dew point with water vapour condensation, are discussed. Experimental results are provided for a large-scale (1.5 m) heat pipe filled with a water/ammonia mixture. These results are utilised in mathematical modelling and optimisation of heat exchanger performance involving heat pipes. The heat transfer process is simulated in a two-stage heat exchanger, where different sections of heat pipes are filled with different working fluids depending on the temperature zones. The optimisation is performed using the minimum entropy production method. The optimal distribution of heat flux density and temperature is determined, considering both design and operational parameters. Numerical examples are provided to demonstrate the performance of the heat recovery system. The results of numerical modelling and optimisation of the design and operating parameters of a two-stage heat exchanger of heat pipes filled with various liquids are presented. The optimal parameters of the heat exchanger are determined using the criterion of minimum entropy production.

Keywords: Heat exchanger; Heat pipes; Deep cooling; Thermodynamic efficiency; Entropy generation; Boiler combustion product

Vol. 46(2025), No. 4, 157–164; doi: 10.24425/ather.2025.156846

Cite this manuscript as: Redko, A., Ujma, A., Redko, O., Redko, I., Zadiranov, V., & Zaika, V. (2025). Optimisation of heat pipe heat exchangers with deep cooling of boiler flue gas based on entropy generation minimisation method. *Archives of Thermodynamics*, 46(4), 157–164.

1. Introduction

Heat exchangers are critical components of boiler systems, contributing significantly to their energy efficiency, environmental performance, and economic viability. The scientific literature extensively discusses the theoretical foundations and criteria for selecting working fluids and components [1−5]. Applications of heat exchangers based on heat pipes are well documented in various industries, including steel [6] and ceramics [7]. Thermosiphon heat pipes, owing to their high thermal capacity, have also been explored for use in city gate station heaters [8,9]. Combustion product heat recovery can increase the thermal power output of boilers by 10–12%. Combustion gases typically contain 10–20% water vapour. When cooled below 50–55°C, more than

Nomenclature

$A_{0.ev}$ – internal ribbed surface area of the heat pipe in the evaporation zone, kW/K
$A_{r,ev}$ – external ribbed surface area of the heat pipe in the evaporation zone, kW/K
$A_{0,c}$ – internal/external surface area of the heat pipe in the condensation zone, kW/K
c_{pg} – specific heat of combustion products, J/(kg K)
D – outer diameter of the pipe ribbing, m
E – rib efficiency factor
h_p – rib height, m
K_{ir} – irrigation density, kg/(m^2 h)
l – length of thermosiphon, m
m – weight of the device, kg
$\dot{m}_g$ – exhaust gas consumption, m^3/h
N – number of rows of the HP
Pr – Prandtl number
P_v/P_g – relative volume concentration of water vapour at the interface
Δp – pressure losses in the gas duct, Pa
ΔP – aerodynamic resistance of the heat exchanger for gas, Pa
Q – the amount of heat transferred, kW
Q_g^* – amount of heat transferred by convection, kW
Re – Reynolds number
r_v – relative volume concentration of water vapour in the combustion product flow, %
S_p – rib pitch on the heat pipes, m
ΔS – change in the entropy of heat carriers, kW/K
ΔS_{heat} – entropy change due to heat transfer, kW/K
$\Delta S_{\Delta p}$ – entropy change due to viscous friction, kW/K
ΔS_c – change in entropy due to condensation of water vapour on the surface of heat pipes in the evaporation zone, kW/K
t_{c1c} – temperature of the inner surface of the thermosiphon in the condensation zone, °C
t_{c2c} – temperature of the surface of the thermosiphon in the condensation zone, °C
t_g – temperature of gas, °C
t_s – temperature of the working fluid in the heat pipe, °C
t_w – temperature of water, °C
T_1, T_2 – heat carrier temperatures, K
W_1, W_2 – heat capacity rate, kW/K
X_1,… X_5 – coded dimensionless variables that take values of ±1
Z – distance between the edges of the adjacent heat pipes, m

Greek symbols

α_{1ev} – heat transfer coefficient from the inner surface of the heat pipe wall to the working heat carrier, W/(m^2 K)
α_{1c} – heat transfer coefficient from the working fluid to the heat pipe inner wall in the condensation zone, W/(m^2 K)
α_{2av} – average heat transfer coefficient of the ribbed pipe bundle when washing effluent gases by the cross-flow, W(/m^2 K)
α_{2c} – heat transfer coefficient from the heat pipe wall to the heated water in the condensation zone, W/(m^2 K)
α_{2ev} – heat transfer coefficient from gas to the ribbed ‘dry’ evaporation zone surface, W/(m^2 K)
α_r – heat transfer coefficient on the rib surface, W/(m^2 K)
δ – fin thickness, m
η_{opt} – efficiency of the optimum heat exchanger, %
λ – thermal conductivity, W/(m K)
ρ – density, kg/m^3
σ – entropy generation, kW/K
φ – ribbing surface ratio
ψ – additional geometric coefficient

Subscripts and Superscripts

c – condensation
ev – evaporation
g – gas
in – inlet
out – outlet
r – rib
w – water

Abbreviations and Acronyms

HP – heat pipe

70–80% of this moisture condenses. The resulting dehumidified combustion gases exit the chimney with increased operational reliability, as there is minimal risk of condensation forming within the flue.

The temperature at the outlet of a heat exchanger is limited by economic considerations. For optimal operation, the efficiency of the heat exchanger should range between 0.55 and 0.65, depending on the gas flow rate and pressure drop. The complexity of heat and mass transfer processes in condensate-based heat exchangers necessitates more advanced modelling and optimization techniques. While literature offers a variety of methods for designing condensation surface heat exchangers, practical applications often rely on empirical relationships [10]. However, these relationships require adjustments when applied to deep flue gas cooling in vertical heat pipes filled with low-temperature working fluids. Under specific conditions, the influence of non-analogous heat and mass transfer mechanisms can be neglected, enabling simplified engineering models.

Studies on condensation of water vapour in combustion gases containing non-condensable components (e.g. CO_2, NO_x) assume that cross vapour flow effects are minimal. Furthermore, the thermal resistance of the vapour film is significantly greater than that of the gas mixture, and can thus be neglected. This allows for using the film condensation mechanism in modelling and optimization. Consequently, the external heat transfer coefficients in both the dry and condensation zones of ribbed heat pipes can be calculated using different correlations. A comparison of various empirical relationships is presented in [11−14].

In the mathematical model developed for this study, water flows longitudinally in a multi-pass configuration, while combustion gases flow counter-currently in a single pass. The heat pipes have vertically oriented evaporation and condensation zones with different lengths ($l_{ev} > l_c$), and are equipped with spiral cross ribs. The heat recovery system is of the ‘liquid-gas’ type, heating water from 5–10°C to 55–65°C.

2. Materials and methods

Figures 1 and 2 show a diagram of the heat exchanger. The heat pipes are fixed into the exchanger’s tube sheet and arranged in

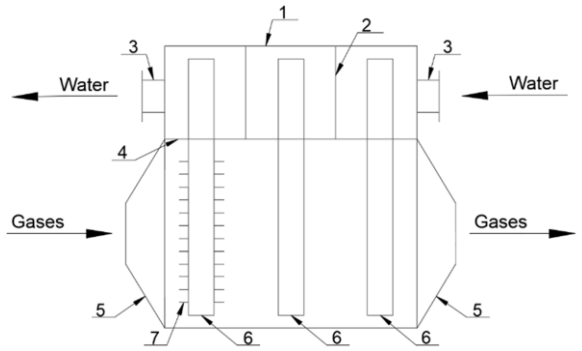

Fig. 1. Longitudinal section of the heat-pipe heat exchanger: 1 − water-side baffle, 2 − subsequent water-side baffle (forming alternating cross-counterflow passes), 3 − water nozzles (inlet/outlet), 4 − tube sheet, 5 − shell (flue-gas duct), 6 − heat pipes (thermosiphons), 7 − fins on the evaporator section of the heat pipe.

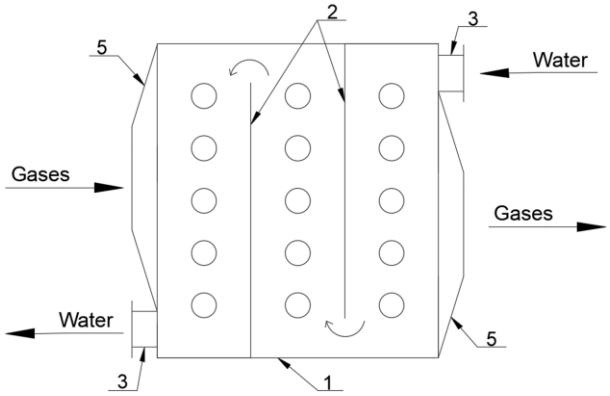

Fig. 2. Longitudinal section of the heat-pipe heat exchanger (tube-sheet/front view): 1 − water-side baffle, 2 − subsequent water-side baffle (forming alternating cross-counterflow passes), 3 − water nozzles (inlet/outlet), 5 − shell (flue-gas duct).

rows along the flue gas flow. The number of tubes was varied both across the width (6–8) and along the length (10–15), depending on the required thermal duty. The condenser sections of the heat pipes are washed by water in a cross-counterflow, multi-pass arrangement formed by baffles. The condenser section of each heat pipe is shorter than its evaporator section. The evaporator sections are finned with annular (or helical-ribbon) fins.

The mathematical model of a heat exchanger employing heat pipes includes the overall energy balance equation, as well as individual heat transfer equations corresponding to each elementary stage of the heat exchange process from gas to liquid. These stages include:

- the heat transfer from gas to liquid − the working heat carrier of the heat pipe in the evaporation zone:

$$Q = \frac{(t_g - t_s)}{R_{ev}(t_s, Q)}, \tag{1}$$

$$R_{ev}(t_s, Q) = \frac{1}{\alpha_{2ev} A_{r.ev}} + \frac{\delta_w}{\lambda_w A_{0.ev}} + \frac{1}{\alpha_{1ev} A_{0.ev}}, \tag{2}$$

- the heat transfer from the heat-carrier fluid of the heat pipe to the inner wall of the pipe in the condensation zone:

$$Q = \alpha_{1c} A_{0.c} (t_s - t_{c1c}), \tag{3}$$

- the heat conduction through the wall of the heat pipe in the condensation zone:

$$Q = \frac{\lambda_w}{\delta_w} A_{0.c} (t_{c1c} - t_{c2c}), \tag{4}$$

- the heat transfer from the outer wall of the heat pipe to the heated water:

$$Q = \alpha_{2c} A_{0.c} (t_{c2c} - t_w), \tag{5}$$

where t_{c1c} and t_{c2c} represent the temperatures of the inner and outer surfaces of the thermosiphon in the condensation zone, respectively, Q denotes the amount of heat transferred, t_s is the temperature of the working fluid inside the heat pipe, t_g and t_w are the temperatures of gas and water, respectively, $A_{0.ev}$ and $A_{r.ev}$ are the internal and external ribbed surface area of the heat pipe in the evaporation zone, $A_{0.c}$ is the surface area of the heat pipe (both internal and external) in the condensation zone, α_{2c} and α_{2ev} are the heat transfer coefficients from the heat pipe wall to the heated water in the condensation zone and from the combustion gases to the ribbed surface in the evaporation zone, respectively, α_{1c} stands for the heat transfer coefficient from the working fluid to the heat pipe inner wall in the condensation zone, α_{1ev} represents the heat transfer coefficient from the inner surface of the heat pipe wall to its working fluid.

The system of Eqs. (1)–(5) includes four unknown variables (t_{c1c}, t_{c2c}, t_s, Q). The system is nonlinear due to the dependence of the heat transfer coefficient on the heat flow rate.

The system of Eqs. (3)–(5) can be transformed to the form

$$t_{c1c} - \frac{Q\delta_w}{\lambda_w A_{0.c}} = t_w + \frac{Q}{\alpha_{2c} A_{r.c}}, \tag{6}$$

$$t_{c1c} = t_s - \frac{Q}{\alpha_{1c} A_{0.c}}, \tag{7}$$

where Q is determined iteratively using Eq. (1), while temperatures t_s and t_{c1c} are obtained from Eqs. (6) and (7), respectively.

The total heat flux transferred to the heat pipes and directed into the thermosiphon is given by

$$Q = Q_g + Q_c. \tag{8}$$

The heat balance equation for the evaporation zone of the heat pipe (convective heat transfer component) is given as follows:

$$Q_g = \alpha_{2ev} A_{2ev} (t_g - t_{av}). \tag{9}$$

To determine the heat transfer coefficient α_{2ev}, the following empirical correlations are used:

$$\alpha_{2ev} = \alpha_{2av} \frac{A_r E \psi + A_0}{A_r}, \tag{10}$$

where E is the rib efficiency factor, A_0 is the area of a smooth surface, α_{2av} is the average heat transfer coefficient for a ribbed pipe bundle subjected to cross-flow of exhaust gases [15]:

$$\alpha_{2av} = 0.33 c_z c_s \left(\frac{\lambda_g}{l}\right) \varphi^{-0.5} \mathrm{Re}^{0.6\varphi^{0.07}} \mathrm{Pr}^{0.33} \left(\frac{\mathrm{Pr}_g}{\mathrm{Pr}_{2c}}\right)^{0.25}, \tag{11}$$

where c_z and c_s are correction factors depending on the number of transverse rows of pipes in the bundle and on the pipe pitch in the bundle, l the length of thermosiphon, Re represents the Reynolds number, Pr is the Prandtl number, Pr_g and Pr_{2c} stand for Prandtl number for gas and condensate, respectively, and φ is the ribbing surface ratio. The latent heat released during water vapour condensation is calculated using the following formula:

$$Q_c = \alpha_{2av} A_{2ev} r_v \frac{R_v}{R_g}\left(r_v - \frac{P_v}{P_g}\right)\frac{1}{c_{pg}}, \qquad (12)$$

where P_v/P_g is the relative volumetric concentration of water vapour at the gas-liquid interface, r_v is the relative volumetric concentration of water vapour in the combustion product flow (with $r_v < 20\%$), R_v and R_g denote the gas constants for vapour and gas, respectively, and c_{pg} denotes the specific heat capacity of the combustion products. A filmwise condensation mechanism for water vapour − representing an approximate analogy between heat and mass transfer − is assumed in the computations. This regime is ensured by the geometric parameters of the ribbed pipe bundles. Specifically, the rib height, thickness and material are selected to satisfy the following conditions:

$$D < 57\times10^{-3}\ \text{m},\ \ S_p > (3.5–4.0)\times10^{-3}\ \text{m},\ \ \varphi < 14,$$

$$\left(\frac{2\alpha_r}{\delta_r\lambda_r}\right)^{\frac{1}{2}} D \le 3.2, \qquad (13)$$

where α_r is the heat transfer coefficient on the rib surface, S_p is the rib pitch and D is the outer diameter of the pipe. The design ensures a rib efficiency factor $E > 0.9$. The critical heat fluxes across the pipe's cross-sectional area were determined according to the method described in [16]. The optimisation technique is described in detail in [17]. The calculation procedure, based on a sequential arrangement of pipe rows, allows for a zone-by-zone evaluation of parameters along the heat exchanger. These parameters include temperature, pressure, the amount of heat transferred, heat pipe power, the quantity of condensate formed, and others. The following parameters were treated as variables: the length of the heat pipe and its evaporation zone, the outer and inner diameters of the heat pipe, the number of pipes per row, the spacing between pipes, the height, thickness and pitch of the ribs, as well as the flow rate and temperature of the combustion products at the inlet, and the flow rate and temperature of the inlet water. The total number of heat pipes (i.e. the overall heat transfer surface area), the temperatures of the heat carriers, the wall temperature and the temperature of the intermediate working fluid inside the heat pipes, as well as the aerodynamic resistance of the combustion gases, the hydraulic resistance on the water side and the total mass of the heat recovery unit, were determined as outcomes of the computational experiment. Irreversible energy losses in the heat recovery unit arise from heat transfer across finite temperature differences, mass transfer during the condensation of water vapour and viscous friction in the flow of the heat carrier.

An experimental setup was developed to validate the analytical relationships used in the mathematical model (Fig. 3). The experimental rig, as shown in the figure, comprises heat pipes

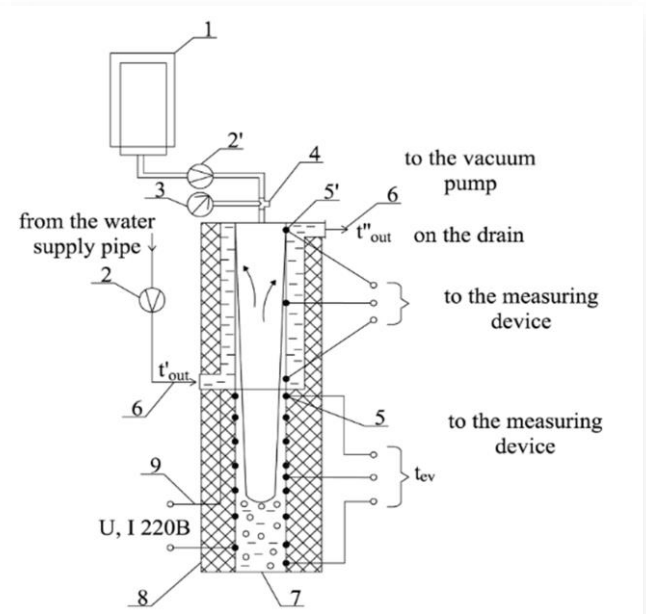

Fig. 3. Scheme of the experimental setup to determine thermal heat pipe capacity: 1 – calibrated measuring tank (graduated vessel) for water flow-rate determination, 2 (2') − flow meters, 3 – manometer, 4 − shut-off valves, 5 (5') − copper-constantan thermocouples, 6 − thermometer; 7 − heat pipe, 8 – insulation, 9 − heating element.

with an evaporator section length of 1000 mm, a condenser section length of 500 mm and an outer diameter of 50 mm. Thermocouples were affixed to the external surface of each heat pipe. An ammonia-water working fluid was employed at concentrations of 10%, 25%, and 40%. The objective of the experiments was to determine the thermal power (heat transfer rate) of the heat pipe of this design. Heat was supplied by an electric heater. The useful thermal power was determined by measuring the water mass flow rate and the temperature difference between the shell outlet and inlet in the water-circulation loop. It was found that the thermal power of the heat pipe of the studied design is 5−6 kW. The experimental results were used as estimation inputs for modelling the heat exchanger parameters.

Experimental studies were conducted to evaluate the thermal capacity of a heat pipe (HP) filled with ammonia-water solution (25% NH_3) at surface temperatures ranging from 40°C to 120°C. The heat is supplied by an electric heater (9) mounted on the surface of the HP in the evaporation zone of the working fluid. In the condensation zone, heat is removed by water flowing through a casing mounted around the HP. The water temperature at the inlet and outlet of the casing is measured using a thermometer (6), while the water flow rate is monitored with a flow meter (2). The surface temperature of the thermosiphon in both the evaporation and condensation zones is recorded using copper-constantan thermocouples fixed on the respective surfaces (positions 5 and 5′). The pressure of the working fluid is measured using a manometer (3), and its temperature is determined based on the saturated vapour pressure.

Figure 4 presents a comparison between the experimental results and the calculated thermal power output of the HP. The thermal power of the heat pipe (HP) was measured as a function

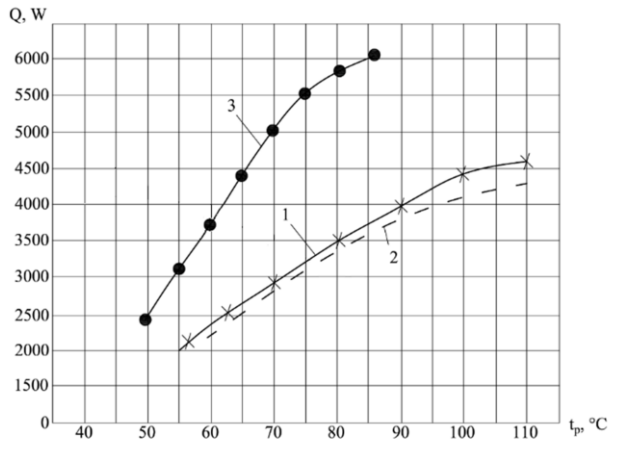

Fig. 4. Heat pipe power as a function of the working fluid temperature: 1 – ammonia-water with a 25% NH_3 concentration (experimental data), 2 – ammonia-water with a 25% NH_3 concentration (calculated data), 3 – ammonia-water with a 40% NH_3 concentration (calculated data).

of the vapour temperature of the working fluid (t_p). A comparison between the experimental and calculated values confirmed the qualitative accuracy of the modelled HP power functions at different ammonia concentrations. In particular, the HP filled with an ammonia-water solution containing 40% NH_3 demonstrated higher thermal efficiency within the temperature range of 40–120°C compared to heat pipes with other concentrations.

A parametric study was carried out to investigate the influence of input variables on the number of rows in the apparatus (assuming 6–8 thermosiphons per row), aerodynamic resistance and the total mass of the heat recovery unit. Pareto-optimal solutions were obtained using a multi-criteria optimisation algorithm. The optimisation was performed with a program based on the Sobol sequences method (also called the LPτ-sequence method or (*t,s*) sequences in base 2), which systematically probes the factor space through uniformly distributed experimental design points. The optimisation methodology, described in detail in [17−19], employs LPτ-search [20] to generate structured multifactor simulation plans. This technique, belonging to the class of Monte Carlo methods, enables the construction of stable regression models and helps reduce estimate variance and standard error. The computational experiments were designed using the Multicrit software package. The system as a whole is intended to identify efficient configurations of the heat exchanger by regenerating sets of input parameters within specified bounds. The variation ranges for the key factors are as follows: thermosiphon length l = 1.0−1.1 m; rib pitch on the HP S_p = 0.004−0.008 m, rib height h_p = 0.025−0.035 m, exhaust gas flow rate $\dot{m}_g$ = 8200−9200 m^3/h, distance between adjacent HPs Z = 0.006−0.012 m.

The solution to the multi-criteria optimisation problem yields a set of effective Pareto-optimal points, which cannot be directly compared with one another across all criteria. Therefore, the final decision must be made subjectively, based on engineering judgment or project-specific priorities. In the optimisation of the heat recovery device, the goal is to minimise the following criteria: N is the number heat pipe rows; ΔP is pressure difference of the heat exchanger to gas flow, m is the weight of the device, ΔS is the entropy change of the heat carriers.

The energy balance equation is extended by incorporating an entropy balance equation, in accordance with the methodology outlined in [21]:

$$\sigma = \Delta S_{heat} + \Delta S_c + \Delta S_{\Delta p}, \quad (14)$$

where ΔS_{heat} is the entropy change associated with heat transfer, $\Delta S_{\Delta p}$ is the entropy change resulting from viscous friction in the flow of the heat carrier and ΔS_c is the change in entropy due to vapour condensation on the surface of the heat pipes in the evaporation zone.

Equation (14) can be written as

$$\sigma = Q_g\left(\frac{1}{T_1}-\frac{1}{T_2}\right) + Q_c\left(\frac{1}{T_1}-\frac{1}{T_2}\right) + \frac{\dot{m}_1 \Delta p}{\rho_0 T_1}, \quad (15)$$

where T_1 and T_2 are the heat carrier temperatures, Δp represents pressure losses in the gas duct, $\dot{m}_1$ is the mass flow rate and ρ_0 is the density of combustion products.

3. Results and discussion

The regression equations are derived from the results of a computational experiment based on a three-level Hartley design, involving five factors and a total of 27 experimental runs.

The experimental plan includes a core structure in the form of a fractional factorial design of type '25-1' (16 basic experiments, 10 'star' points and 1 'zero' point).

As a result of the computational experiment, the following regression models were developed:

$$N = 9.3333 + 0.222222X_1 + 1.83333X_2 - 0.333333X_3 + 0.222222X_4, \quad (16)$$

$$\Delta P = 94.22 - 6.61111X_1 - 8.32222X_2 + 34.0444X_3 - 12.25X_4 + 7.61111X_5 + 6.96X_2^2 + 10.36X_3^2 + 2.825X_1X_3 + 6.1625X_3X_4, \quad (17)$$

where X_1, X_2, X_3, X_4, X_5 are coded dimensionless variables that take values of ±1:

$$X_1 = \frac{l_{ev}+1.05}{0.05}, X_2 = \frac{S_p-0.006}{0.002}, X_2 = \frac{h_p-0.03}{0.005},$$

$$X_4 = \frac{Z-0.009}{0.003}, X_2 = \frac{\dot{m}_g-8700}{500}.$$

The influence of various input parameters on the thermal power output, aerodynamic resistance and total mass of the device has been evaluated.

Designing the heat exchanger requires establishing quantitative relationships between the selected heat and mass transfer indicators and the initial parameters, as well as optimising the thermal characteristics of the system. The objective of the computational experiment was to evaluate the influence of input parameter variations on the required heat transfer surface area and the aerodynamic resistance of the system, under the constraint of a fixed thermal power and the condition of minimum entropy production. A multi-criteria optimisation program based on the

probing of the factor space using uniformly distributed sequences was applied [20].

The results show that the thermal performance of the heat exchanger is strongly influenced by the choice of working fluid in each stage of the device. The selection of the working fluid determines the temperature distribution of the heat carrier along the apparatus, the local heat transfer coefficient and the resulting heat flux density. At combustion gas temperatures of 150–130°C, optimal working fluids were found to be: water in the first stage and a water-ammonia mixture in the second stage.

Simulation results indicate that the condensation of water vapour significantly increases the heat flux density. In particular, the share of condensation heat in the total heat transfer increases to 64%, while the water vapour content in the combustion gases decreases from 18% to 10–12%.

Figure 5 shows the variation of entropy production as a function of the heat capacity rate of the combustion products. As it can be seen, at a constant power of a heat exchanger the decrease in the temperature of combustion products and the increase in their flow rate result in reducing the entropy production.

Numerical simulations were carried out for a two-stage heat

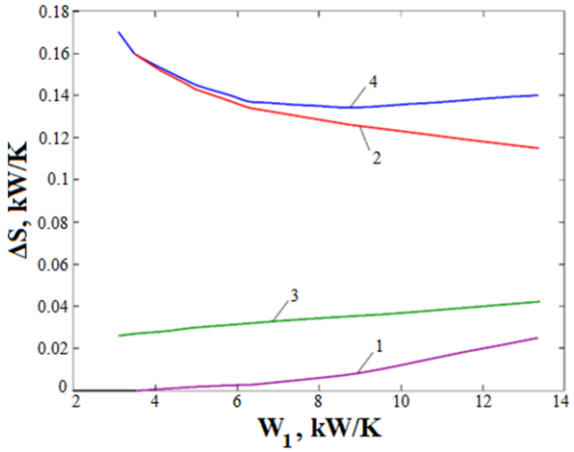

Fig. 5. Entropy production vs. gas heat capacity rate: 1 − mechanical, 2 − thermal, 3 − at the condensation of water vapour, 4 − total.

recovery unit utilising heat pipes (thermosiphons) filled with two different working fluids in the first and second stages. Water, ammonia-water solution, methanol and isobutane (C_4H_{10}) were considered as potential working fluids for the heat pipes. The results show that the heat exchange surface area for a heat recovery unit with heat pipes filled with water is significantly smaller (by approximately 39–40%) compared to heat pipes filled with isobutane. However, the thermal power increases in a heat recovery unit designed according to a two-stage thermal scheme: the first stage consists of 3 rows of heat pipes (thermosiphons) filled with methanol and the second stage consists of 18 rows of thermosiphons filled with isobutane, or, the first stage consists of 3 rows of heat pipes filled with methanol and the second stage consists of 10 rows of thermosiphons filled with ammonia water. The distribution of heat pipes thermal power along the length of the heat recovery unit is shown in Fig. 6.

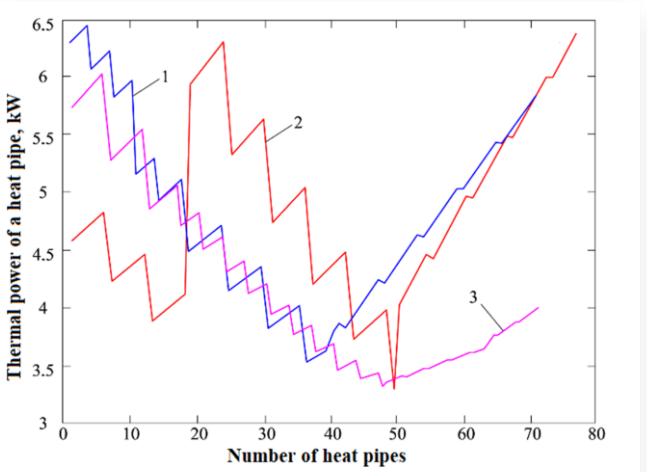

Fig. 6. Distribution of thermal power of heat pipes along the length of the heat recovery unit: 1 – up to the 19th thermosiphon – methanol and in others – isobutane, 2 – up to the 19th thermosiphon – methanol and in others – ammonia-water,
3 – ammonia-water in all thermosiphons.

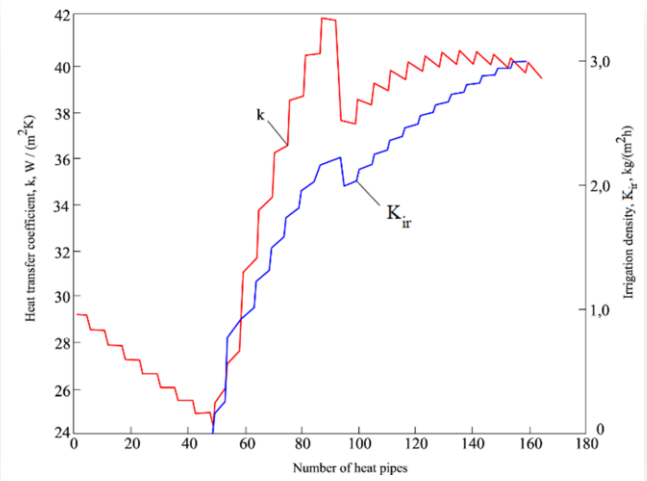

Fig. 7. Distribution of the heat transfer coefficient and irrigation density along the length of the heat recovery unit.

Figure 7 presents the variation of the heat transfer coefficient and water vapour concentration along the length of the heat recovery unit. The observed increase in thermal power output of the heat pipes in the second stage is attributed to the condensation of water vapour.

The accuracy of the computational model was verified using experimental data for the irrigation density (K_{ir}) defined as the amount of water vapour condensed per square meter of heat exchange surface per hour. Figure 7 also shows the distribution of the irrigation density K_{ir} along the length of the heat exchanger with a total heat exchange surface area of 443.52 m^2. At a combustion gas flow rate of 10×10^3 m^3/h, the irrigation coefficient varies from 0 to 2.8 kg/(m^2 h).

According to experimental data [22], typical values of K_{ir} range from 2 to 4 kg/(m^2 h). For a steam DE-type boiler, the measured mass of condensate collected in the apparatus is 260–

Table 1. Results of heat exchanger parameter optimisation considering water vapour condensation.

Gas temperature at the inlet, °C	Gas flow rate, m³/h	Heat capacity rate, kW/K	Thermal power/Q_g^*, kW/kW	Water temperature at the inlet, °C	Gas temperature at the outlet, °C	Heat transfer capacity ($k \times A$), kW/K	Pressure losses, Pa	Entropy production, kW/K (therm./mech./tot.)
130	8000	3.10	301/244	41.0	50.6	4.64	59	0.170(0.026)/0.00/0.170
120	9000	3.48	298/237	40.6	51.2	4.86	72	0.160(0.027)/0.00/0.160
100	13000	4.99	299/230	40.7	53.6	5.57	133	0.143(0.030)/0.002/0.145
90	16500	6.32	299/223	40.6	54.6	6.04	200	0.134(0.032)/0.003/0.137
80	23000	8.79	299/214	40.7	55.6	6.70	352	0.126(0.035)/0.008/0.134
70	35000	13.34	298/192	40.5	55.6	7.61	721	0.115(0.042)/0.025/0.140

Q_g^* is the amount of heat being transferred by convection.

Table 2. Results of heat exchanger parameter optimisation without water vapour condensation.

Gas temperature at the inlet, °C	Gas flow rate, m³/h	Heat capacity rate, kW/K	Thermal power, kW	Water temperature at the inlet, °C	Gas temperature at the outlet, °C	Heat transfer capacity ($k \times A$), kW/K	Pressure losses, Pa	Entropy production, kW/K (therm./mech./tot)	Entropy production, kW/K*
140	8200	3.18	302	41.0	44.2	4.68	124	0.189/0.001/0.190	0.181
130	9400	3.64	300	40.8	47.0	4.78	157	0.181/0.002/0.183	0.174
120	11300	4.36	300	40.8	50.7	4.93	215	0.176/0.003/0.178	0.169
110	14200	5.47	300	40.9	54.7	5.10	318	0.170/0.005/0.175	0.164
100	19000	7.30	299	40.7	58.8	5.29	525	0.163/0.011/0.174	0.159
90	30000	11.50	300	40.8	63.9	5.56	1156	0.158/0.036/0.194	0.147
98	20700	7.95	300	40.8	60.1	5.35	609	0.163/0.013/0.176	0.152
104	16650	6.00	299	40.7	57.0	5.2	418	0.166/0.007/0.173	0.161

*Calculated according to the formula: $\Delta S = W_1 \ln(T_1^{out}/T_1^{in}) + W_2 \ln(T_2^{out}/T_2^{in})$

340 kg/h. The proposed method yields a calculated value of 240 kg/h, confirming high accuracy of the developed model. In this simulation, the working fluid is water up to the 97th thermosiphon and ammonia-water mixture beyond that point (60/40% split). The increase in entropy production due to viscous friction corresponds to a minimum total entropy generation dS_{total} = 0.134 kW/K (as shown in Table 1) at a combustion gas inlet temperature of T_1 = 80°C and a heat capacity rate W_1 = 8.79 kW/K. As W_1 increases, the required heat exchange surface area multiplied by the overall heat transfer coefficient (i.e. the $k \times A$ value) increases from 4.68 to 5.56 kW/K. As can be seen, in the absence of water vapour condensation, entropy production becomes more intensive − by up to 31% − due to increased gas flow rate required to maintain the same thermal power output (Table 2).

The calculated results for the heat exchanger parameters without water vapour condensation are presented in Table 2.

When modelling and optimising thermal parameters of the heat exchanger, the entropy production criterion σ allows for an increase in the outlet temperature T_2 of the heated medium by selecting appropriate values of heat capacity rates W_1 and W_2, as well as by choosing an optimal heat exchange configuration for a given heat transfer surface area. Numerical investigations were conducted to analyse the effect of varying the heat consumption of the heated medium (W_2) on the efficiency of the optimised heat exchanger (η_{opt}).

4. Summary and conclusions

The results of numerical simulation and optimisation of two-stage heat exchanger parameters using heat pipes, with consideration of entropy change, demonstrate the following: operating modes that minimise entropy production lead to reduced irreversible losses in the heat transfer process and enhance the overall energy efficiency of both the heat exchanger and the heat-generating unit. However, the implementation of such modes requires a thorough technical and economic justification − particularly when selecting the heat capacity rate of the combustion products (W_1) − with consideration of relevant economic criteria.

References

[1] Baskakov, A.P., & Il'ina, E.V. (2003). Heat and mass exchange in the deep cooling of the combustion products of natural gas. *Journal of Engineering Physics*, 16(2), 335−342.

[2] Verinchuk, E. (2004). *Modelling of heat-and-mass transfer processes in recuperative condensing heat-utilizers*. PhD thesis, Moscow Energy Institution, Moscow (in Russian).

[3] Redko, I., Redko, A., Pavlovskiiy, S., Redko, O., Burda, Y., & Ujma, A. (2021). Energy efficiency of buildings in the cities of Ukraine under the conditions of sustainable development of centralized heat supply system. *Energy and Buildings*, 247, 110947. doi: 10.1016/j.enbuild.2021.110947

[4] Zhang, Y. (Ed.) (2018). *Heat Pipes: Design, Applications and Technology*. Nova Science Publishers.

[5] Zohuri, B. (2016). *Heat pipe design and technology: Modern applications for practical thermal management* (2nd ed.). Springer. doi: 10.1007/978-3-319-29841-2

[6] Jouhara, H., Almahmoud, S., Chauhan, A., Delpech, B., Bianchi, G., Tassou, S.A., Llera, R., Lago, F., & Arribas, J.J. (2017). Experimental and theoretical investigation of a flat heat pipe heat exchanger for waste heat recovery in the steel industry. *Energy*. 141. 1928−1939. doi: 10.1016/j.energy.2017.10.142

[7] Jouhara, H., Bertrand, D., Axcell, B., Montorsi, L., Venturelli, M., Almahmoud, S., Milani, M., Ahmad, L., & Chauhan, A. (2021). Investigation on a full-scale heat pipe heat exchanger in the ceramics industry for waste heat recovery. *Energy*, 223, 120037. doi: 10.1016/j.energy.2021.120037

[8] Rastegar, S., Kargarsharifabad, H., Behshad Shafii, M., & Rahbar, N. (2020) Experimental investigation of the increasing thermal efficiency of an indirect water bath heater by use of thermosiphon heat pipe. *Thermal Science*, 24(6B), 4277−4287. doi: 10.2298/TSCI190428054R

[9] Azizi, S.H., Rashidmardani, A, & Andalibi, M.R. (2014). Study of preheating natural gas in gas pressure reduction station by the flue gas of indirect water bath heater. *International Journal of Science and Engineering Investigations*, 3(27), 17−22.

[10] Cherepanova, E. (2005). *Cooling combustion products of gaseous fuel in ribbed heat exchangers*. PhD thesis, Ural State Technical University, Ekaterinburg (in Russian).

[11] Isachenko, V.P., Osipova, V.A., & Sukomel, A.S. (1975). *Heat transfer* (3rd ed.). Energiya, Moscow.

[12] Zhukauskas, A. (1982) *Convective transfer in heat exchangers*. Nauka, Moscow (in Russian).

[13] Mikheev, M.A., & Mikheeva, I.M. (1977). *Fundamentals of heat transfer* (2nd ed.). Energiya, Moscow (in Russian).

[14] Labuntsov, D. (1960). Heat exchange during steam condensation on a vertical surface under conditions of turbulent runoff of a condensate film. *Journal of Engineering Physics and Thermophysics*, 3(8), 3−12.

[15] Yudin, V.F. (1982). Heat exchange of cross-ribbed pipes (pp. 46–108). Mashinostroyenie, Leningrad (in Russian).

[16] Bezrodnyi, M.K., Pioro, I.L., & Kostyuk, T.O. (2005). *Transfer processes in two-phase thermosiphon systems. Theory and practice* (2nd ed.). Fact Publishing House, Kiev (in Russian).

[17] Kulikova, N., & Redko, A. (2014). Simulating of heat-transfer processes in two-phase heat-utilizer at heat pipes. *Structure and Environment*, 6(2), 35−43.

[18] Nikolaev, G. (2012). Calculation of operating characteristics of loop heat pipes. *Journal of Young Scientist*, 3, 17−25.

[19] Redko, A., Kulikova, N., Pavlovskiiy, S., & Redko, A. (2018) Simulation and optimization of heat-exchanger parameters of heat pipes by changes of entropy. *Heat Transfer Research*, 49(16), 1545−1557. doi: 10.1615/HeatTransRes.2018019336

[20] Sobol, I.M., & Statnikov, R.B. (1981). *Selecting optimal parameters in multicriteria problems*. Nauka, Moscow (in Russian).

[21] Bejan, A. (2006). *Advanced engineering thermodynamics* (3 ed.) (pp. 101−144, 574−655), John Wiley & Sons, New York. doi: 10.1002/9781119245964

[22] Kudinov, A. (2001) *Energy saving in thermal generating plants.* Ulyanovsk State Technical University, Ulyanovsk.